The Journal of Chemical Physics ARTICLE scitation.org/journal/jcp

Single-file diffusion in a bi-stable potential: Signatures of memory in the barrier-crossing of a tagged-particle

Cite as: J. Chem. Phys. 153, 194104 (2020); doi: 10.1063/5.0025785
Submitted: 18 August 2020 • Accepted: 30 October 2020 •
Published Online: 16 November 2020

Alessio Lapolla and Aljaž Godec[a)]

AFFILIATIONS

Mathematical bioPhysics Group, Max Planck Institute for Biophysical Chemistry, Am Fassberg 11, 37077 Göttingen, Germany

[a)]Author to whom correspondence should be addressed: agodec@mpibpc.mpg.de

ABSTRACT

We investigate memory effects in barrier-crossing in the overdamped setting. We focus on the scenario where the hidden degrees of freedom relax on exactly the same time scale as the observable. As a prototypical model, we analyze tagged-particle diffusion in a single file confined to a bi-stable potential. We identify the signatures of memory and explain their origin. The emerging memory is a result of the projection of collective many-body eigenmodes onto the motion of a tagged-particle. We are interested in the "confining" (all background particles in front of the tagged-particle) and "pushing" (all background particles behind the tagged-particle) scenarios for which we find non-trivial and qualitatively different relaxation behaviors. Notably and somewhat unexpectedly, at a fixed particle number, we find that the higher the barrier, the stronger the memory effects are. The fact that the external potential alters the memory is important more generally and should be taken into account in applications of generalized Langevin equations. Our results can readily be tested experimentally and may be relevant for understanding transport in biological ion-channels.

I. INTRODUCTION

Non-linear stochastic flows are at the heart of thermally driven processes in systems whose potential energy surfaces are characterized by multiple local energy minima. Pioneered by the seminal work of Kramers,[1] the concept of thermally activated barrier-crossing has ever since been applied to diverse phenomena, including chemical reactions,[2–4] tunnel diodes,[5] laser-pumping,[6] magnetic resonance,[7] conformational dynamics and folding of proteins[8–16] and nucleic acids,[17,18] and receptor–ligand binding[19] to name but a few.

From a theoretical point of view, the most detailed and precise results were obtained in the context of relaxation phenomena[20–26] and first passage time statistics[27–34] in Markovian (i.e., memoryless) systems. However, physical observables typically correspond to lower-dimensional projections, and the observed dynamics is Markovian only under quite restrictive conditions on the nature of the projection.[35] Quoting van Kampen: "Non-Markov is the rule, Markov is the exception."[36]

Over the years, the non-Markovian barrier-crossing has therefore received special attention. Most approaches considered a generalized Langevin equation in the underdamped regime with diverse phenomenological memory kernels for the velocity in the high[37–39] and low[40,41] viscosity limits. In the case of diffusion in double-well potentials, unified solutions have been obtained.[42] Seminal results on non-Markovian effects in the crossing of high energy barriers have been obtained by Mel'nikov and Meshkov[43] and were later extended to low barriers by Kalmykov, Coffey, and Titov.[44] Important results on the non-Markovian barrier-crossing have been obtained in the context of condensed-phase dynamics.[45–47] More recent studies of memory effects in bi-stable potentials have been carried out in the context of conformational dynamics of macromolecules[16,48–50] and the role of hydrodynamic memory in surmounting energy barriers,[51] while recent applications involve the interpretation of experiments on the folding of a DNA hairpin.[52]

Quite detailed analytical results have also been obtained for overdamped non-Markovian stochastic flows in bi-stable potentials,

in particular for exponentially correlated noise.[53–57] Characteristic of these studies is that the memory is introduced phenomenologically and/or the systems typically possess slow and fast degrees of freedom. Thereby, integrating out of fast degrees of freedom leads to memory, and timescales similar to, or longer than, the correlation time are of interest.

Here, we are interested in the scenario where the background degrees of freedom (i.e., those that become integrated out) relax on exactly the same time scale as the observable. In particular, we are interested in the relaxation dynamics of a tagged-particle in a single file of Brownian particles confined to a bi-stable potential and investigate the role of the height of the potential barrier. Projecting out particles' positions introduces memory and strongly breaks Markovianity.[35] The more particles' coordinates become integrated out, the stronger Markovianity is broken.[35] A distinguishing characteristic of our approach with respect to the existing literature is, therefore, that we do not introduce memory phenomenologically via a generalized Langevin equation. Instead, the memory arises explicitly as a result of projecting out degrees of freedom in an exactly solvable Markovian many-body system. This is important because any external potential, in general, also affects the memory in the tagged-particle's dynamics.[35,58,59] One, therefore, may *not* employ *ad hoc* memory kernels that are independent of the external potential, except when the potential does not act as background degrees of freedom and the interaction between the background degrees of freedom and the tagged-particle is harmonic or negligibly weak.

Single-file models are generically used to describe strongly correlated, effectively one-dimensional, systems and processes, e.g., biological channels,[60] transport in zeolites,[61] crowding effects in gene regulation,[62,63] superionic conductors,[64] and strongly correlated one-dimensional soft matter systems in general.[65–68] Over the past few years, diverse theoretical studies yielded deep insight about the anomalous tagged-particle diffusion[69–77] and the emergence and meaning of memory.[35,78,79] Single-file diffusion in potential landscapes has been studied by computer simulations.[80]

It is well known that a tagged-particle's diffusion in any homogeneous overdamped system of identically interacting particles with an excluded mutual passage is asymptotically subdiffusive, i.e., the tagged-particle's mean squared displacement asymptotically scales as $\langle x^2\rangle \sim t^{1/2}$ (see, e.g., Ref. 81). However, the manner in which crowding/steric obstruction and particle correlations affect memory in barrier-crossing, and in particular in the relaxation toward equilibrium and how such memory can be inferred and quantified from measurable physical observables, has so far remained elusive. Our results are relevant in the context of search processes of proteins on DNA in the presence of macromolecular crowding involved in transcription regulation and on a conceptual level for transport in ion-channels. More generally, the methodological framework presented here does not require an analytical solution of the problem to be known and can thus also be applied in the analysis of experiments or computer simulations.

In this work, we provide in Sec. II an analytical solution to the problem using the coordinate Bethe ansatz. In Sec. III, we analyze the equilibrium correlation functions and underlying linear memory kernel as a function of the barrier height and number of particles in the single file. Section IV addresses the relaxation to equilibrium from a fixed, non-equilibrium initial condition of the tagged-particle in the "confining" and "pushing" scenario, respectively. We conclude with a brief discussion including potential applications and extensions of our results.

II. THEORY

We consider a single file of N point-particles confined to a box of length of $L = 2\pi$. In the center of the box, there is a square-top energy barrier of width π and height U_b [see Fig. 1(a)]. More precisely, each particle experiences the potential[82,83]

$$U(x) = \begin{cases} 0, & \pi > |x| > \pi/2 \\ U_b, & |x| \le \pi/2 \\ \infty, & \text{otherwise.} \end{cases} \tag{1}$$

The particles move according to overdamped Brownian dynamics but are not allowed to cross. For simplicity and without loss of generality, we set $D = 1$, which is equivalent to expressing time in units of $4\pi^2/D$, and express U in units of thermal energy k_BT, i.e., $U \to U/k_BT$. The probability density of the set of positions $\{x_i\} = \mathbf{x}$ of the N particles evolves according to the many-body Fokker–Planck equation,

$$\left(\partial_t - \sum_{i=1}^{N}\left[\partial_{x_i}^2 + \partial_{x_i}\{\partial_{x_i}U(x_i)\}\right]\right)G(\mathbf{x},t|\mathbf{x}_0) = 0, \tag{2}$$

with the initial condition $G(\mathbf{x},0|\mathbf{x}_0) = \prod_{i=1}^{N}\delta(x_i - x_{0i})$, where the operator in curly brackets $\{\}$ acts only within the bracket. Equation (2) is equipped with the set of external and internal boundary conditions,

$$\begin{aligned} \partial_{x_1}G(\mathbf{x},t|\mathbf{x}_0)|_{x_1=-\pi} = \partial_{x_N}G(\mathbf{x},t|\mathbf{x}_0)|_{x_N=\pi} = 0, \\ (\partial_{x_{i+1}} - \partial_{x_i})G(\mathbf{x},t|\mathbf{x}_0)|_{x_{i+1}=x_i} = 0, \end{aligned} \tag{3}$$

and is solved exactly using the coordinate Bethe ansatz (for technical details, refer to Refs. 35, 79, and 84). In a nutshell, the Bethe ansatz solution exploits the intuitive fact that a trajectory of N identical non-crossing Brownian particles is *identical* to that of an ideal Brownian gas if we re-label the particle indices such that that they are ordered at all times. As a result, one can construct the probability density of the set of particles' positions $\mathbf{x}$ by a suitable permutation of the products of probability densities of individual, non-interacting particles. In turn, an eigenfunction expansion of the many-body Fokker–Planck operator can be obtained by permuting products of single-particle eigenspectra, which is what we exploit in the present article. The resulting Bethe many-body Green's function reads

$$G(\mathbf{x},t|\mathbf{x}_0) = \sum_{\mathbf{k}}\Psi_{\mathbf{k}}^R(\mathbf{x})\Psi_{\mathbf{k}}^L(\mathbf{x}_0)e^{-\Lambda_{\mathbf{k}}\tau}, \tag{4}$$

where $\Psi_{\mathbf{k}}^L(\mathbf{x})$ and $\Psi_{\mathbf{k}}^R(\mathbf{x})$ are the so-called left and right Bethe eigenfunctions, respectively, defined as

$$\Psi_{\mathbf{k}}^{L,R}(\mathbf{x}) \equiv \mathcal{N}^{1/2}\hat{O}_{\mathbf{x}}\sum_{\{\mathbf{k}\}}\prod_{i=1}^{N}\psi_{k_i}^{L,R}(x_i), \tag{5}$$

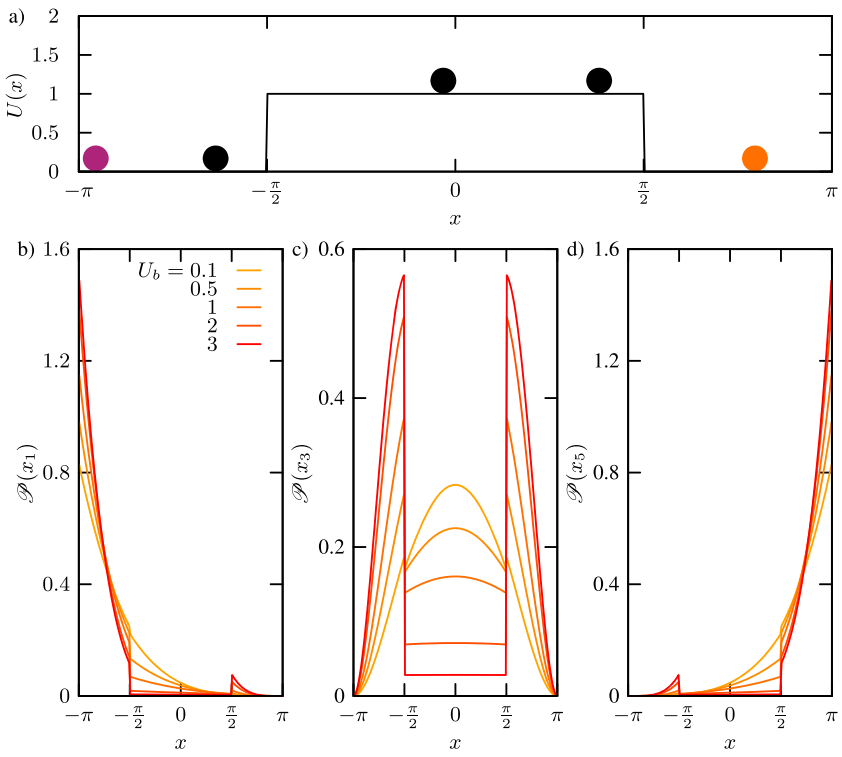

FIG. 1. (a) Schematic of the potential $U(x)$ defined in Eq. (1); single file with $N = 5$ particles. Throughout this work, we either tag the first (magenta stands for $i = 1$) or the last (orange stands for $i = N$) particle. (b)–(d) depict the equilibrium probability distribution $\mathscr{P}_{\rm eq}(x_i)$ for $i = 1$ (b), $i = 3$ (c), and $i = 5$ (d) in a single file with $N = 5$ for different barrier-heights U_b, respectively.

where $\psi_n^{L,R}(x)$ are the orthonormal eigenfunctions of the single-particle problem (given in the Appendix), the sum over $\{\mathbf{k}\}$ refers to the sum over all permutations of the multiset $\mathbf{k}$, and $\mathscr{N}$ is the number of these permutations $\mathbf{k}$. $\Lambda_{\mathbf{k}} = \sum_{i=1}^{N} \lambda_{k_i}$ refers to the Bethe eigenvalue with multi-index $\mathbf{k} = \{k_i\}$, $i \in [1, N]$, and $\hat{O}_{\mathbf{x}}$ is the particle-ordering operator, which ensures that $x_1 \le \cdots \le x_i \le \cdots \le x_N$. Moreover, λ_n refer to the eigenvalues of the respective one-body problem, given by[82,83]

$$\lambda_n = \begin{cases} \dfrac{n^2}{4}, & \mathrm{mod}\,(n,4) = 0, \\ \left(\dfrac{n-1}{2} + \nu\right)^2, & \mathrm{mod}\,(n,4) = 1, \\ \dfrac{n^2}{4}, & \mathrm{mod}\,(n,4) = 2, \\ \left(\dfrac{n+1}{2} - \nu\right)^2, & \mathrm{mod}\,(n,4) = 3, \end{cases} \tag{6}$$

where $\nu = 2\arctan(\mathrm{e}^{-U_b/2})/\pi$ and $\mathrm{mod}(k, l)$ stands for the remainder of the division k/l.

We are interested in the non-Markovian probability density of x_i and the position of the ith tagged-particle under the condition that the initial positions of the remaining particles are drawn from those equilibrium configurations that contain particle i at x_0, which reads (for a derivation, see Refs. 35, 79, and 84)

$$\mathscr{G}(x_i, t|x_{0i}) = V_{\mathbf{00}}^{-1}(x_{0i}) \sum_{\mathbf{k}} V_{\mathbf{0k}}(x_i) V_{\mathbf{k0}}(x_{0i}) \mathrm{e}^{-\Lambda_{\mathbf{k}} t}, \tag{7}$$

where the "overlap-elements" $V_{\mathbf{kl}}(x_i)$ are defined as[84]

$$V_{\mathbf{kl}}(x_i) = \frac{m_{\mathbf{l}}}{N_L! N_R!} \sum_{\{\mathbf{k}\}} \sum_{\{\mathbf{l}\}} \psi_{k_i}^R(x_i) \psi_{l_i}^L(x_i) \prod_{n=1}^{i-1} L_n(x_i) \prod_{m=i+1}^{N} R_m(x_i), \tag{8}$$

with $m_{\mathbf{l}}$ being the multiplicity of the multiset $\mathbf{l}$, and $N_L = i - 1$ and $N_R = N - i$ are the number of particles to the left and right of the tagged-particle, respectively. In Eq. (8), we introduced the auxiliary functions

$$L_n(x) = \int_{-\pi}^{x} dz \psi_{l_n}^L(z) \psi_{k_n}^R(z), \quad R_n(x) = \int_{x}^{\pi} dz \psi_{l_n}^L(z) \psi_{k_n}^R(z). \tag{9}$$

Note that the equilibrium probability density of the tagged-particle's position is given by [see Eq. (7)] $\mathscr{P}_{\rm eq}(x_i) \equiv \lim_{t\to\infty} \mathscr{G}(x_i, t|x_{0i}) = V_{\mathbf{00}}(x_i)$ and is depicted for various values of U_b in Figs. 1(b)–1(d). Intuitively, as U_b increases, particles become expelled from the barrier.

In Ref. 84, we have developed an algorithm designed to efficiently cope with the combinatorial complexity of the implementation of the analytical solution in Eq. (7). Due to the piece-wise constant nature of the potential $U(x)$ in Eq. (1), all integrals (9) can be computed analytically. As the resulting expressions are lengthy, we do not show them here. Instead, they are readily implemented in an extension of the code published in Ref. 84 (see the supplementary material).

III. LINEAR CORRELATIONS AT EQUILIBRIUM

First, we consider linear correlations at equilibrium and limit the discussion in the reminder of this paper to tagging the first or last particle (i.e., throughout, we set $i = 1$ or $i = N$). That is, we are interested in the normalized positional autocorrelation function of a tagged-particle, defined as

$$C_i(t) = \frac{\langle x_i(t)x_i(0)\rangle - \langle x_i\rangle^2}{\langle x_i^2\rangle - \langle x_i\rangle^2}, \tag{10}$$

where the covariance of the position is defined as

$$\langle x_i(t)x_i(0)\rangle \equiv \int_{-\pi}^{\pi} dx_i \int_{-\pi}^{\pi} dx_{0i}\, x_i x_{0i} \mathscr{G}(x_i, t|x_{0i})\mathscr{P}_{\rm eq}(x_{0i}) \tag{11}$$

and $\langle x_i^n\rangle = \int_{-\pi}^{\pi} dx_i\; x_i^n \mathscr{P}_{\rm eq}(x_i)$. The above integrals have been performed numerically by means of Gauss–Kronrod quadrature.[85] Note that Eq. (10) alongside Eqs. (5)–(9) necessarily implies the structure $C_i(t) = \sum_{\mathbf{k}\neq\mathbf{0}} a_{\mathbf{k}} e^{-\Lambda_{\mathbf{k}} t}$ with $\sum_{\mathbf{k}\neq\mathbf{0}} a_{\mathbf{k}} = 1$, where all $a_{\mathbf{k}} \geq 0$.[86] The results for $C_1(t)$ as a function of the barrier height U_b are depicted in Fig. 2. Since $U(x)$ is symmetric, the autocorrelation functions of the first and last particles coincide, i.e., $C_1(t) = C_N(t)$.

The autocorrelation of an isolated particle (i.e., $N = 1$) in Fig. 2(a) displays for a given value of U_b to a good approximation an exponential decay with rate $\Lambda_{\mathbf{1}} = \lambda_1$ given by Eq. (6). This reflects that positional correlations decay predominantly due to barrier-crossing. Conversely, as the number of particles increases, $C_1(t)$ decays on multiple timescales [see Fig. 2(b)] and develops an "anomalous" shoulder on shorter timescales[78] whose span increases with the barrier height U_b. A comparison of $C_1(\Lambda_1^{-1})$ reveals that the relative decay of correlations from the relaxation time $\tau_{\rm rel} \equiv \Lambda_1^{-1}$ onward is substantially reduced for about a factor of 2 compared to the isolated particle case. $\tau_{\rm rel}$ denotes the timescale on which the system reaches equilibrium from any initial condition. Note that (i) $C_1(t)$ measures relative correlations, and (ii) according to Eq. (7) (terminal), relaxation roughly corresponds to the particles individually crossing the barrier several times. It is also important to note that the natural timescale of a tagged-particle is set by the average collision time[35,79] $\tau_{\rm col} = 1/N^2$, which decreases with an increase in N. That is, in units of the average number of collisions, $t \to t/\tau_{\rm col}$ correlations decay more slowly for larger N.

A common means to quantify the extent of correlations found in the literature is the so-called *correlation time* T_c,[25,26,44,87] and it should be compared with the actual relaxation time $\tau_{\rm rel}$,[88]

$$T_c = \int_0^{\infty} dt C_i(t),\;\; \tau_{\rm rel} \equiv \Lambda_1^{-1} = \left(\frac{2}{\pi}\arctan(e^{-U_b/2})\right)^{-2}, \tag{12}$$

where we note that for high barriers, i.e., $U_B \gg 1$, the relaxation time follows the expected Arrhenius scaling $\tau_{\rm rel} \simeq 4e^{U_b}/\pi^2$. In Fig. 3(a), we depict the correlation time for the leftmost particle in units of $\tau_{\rm col}$ as a function of the barrier height U_b for different N. For an isolated particle, $T_c = T_c^{\rm isolated}$ agrees very well with $\tau_{\rm rel}$ for all values of U_b, confirming the idea that $C(t)$ decays to a very good approximation as a single exponential. Note that for systems obeying detailed balance, the mathematical structure of $C_i(t)$ trivially implies a shorter correlation time as soon as $C_i(t)$ decays on multiple timescales if the longest timescale $\Lambda_{\mathbf{1}}^{-1}$ is the same. This is particularly true when comparing $C_i(t)$ of a tagged-particle in a single file with an isolated particle. Namely,

$$T_c = \sum_{\mathbf{k}\neq\mathbf{0}} a_{\mathbf{k}}/\Lambda_{\mathbf{k}} \leq \sum_{\mathbf{k}\neq\mathbf{0}} a_{\mathbf{k}}/\Lambda_{\mathbf{1}} = \Lambda_{\mathbf{1}}^{-1} \approx T_c^{\rm isolated}. \tag{13}$$

Therefore, the interpretation of T_c should always be made cautiously and in the particular case of tagged-particle diffusion in a single file is not meaningful if we consider T_c on an absolute scale. However, it becomes somewhat more meaningful on the natural timescale, i.e., when time is expressed in terms of the average number of interparticle collisions (see also Ref. 35). Inspecting $C_1(t)$ on this natural time scale, we find in Fig. 3(a) that the tagged-particle on average undergoes more collisions before it decorrelates for larger values of N, and this number increases with an increase in U_b.

Moreover, as N increases, the space explored by a tagged-particle becomes progressively more confined[35] rendering the correlation time T_c on an absolute timescale also intuitively shorter. Indeed, in Fig. 3(b), we depict the ratio T_c/Λ_1^{-1}, which decreases with an increase in N for any barrier height U_b. Note that Λ_1^{-1} is independent of N and the breaking of Markovianity (reflected, e.g., in the violation of the Chapman–Kolmogorov semi-group property[35]) is encoded entirely in the overlap elements $V_{\mathbf{0k}}$, $V_{\mathbf{k0}}$. For systems with microscopically reversible dynamics, $T_c/\Lambda_1^{-1} < 1$ quite generally implies that relaxation evolves on multiple timescales. Thus, the results in Fig. 3(b) suggest, in agreement with intuition, that more and more timescales are involved in the relaxation of a tagged-particle's position in equilibrium as we increase N. In other words, on the level of linear correlations' signatures of memory of the initial conditions of "latent"/background, particles are reflected in the multi-scale relaxation of $C_1(t)$.

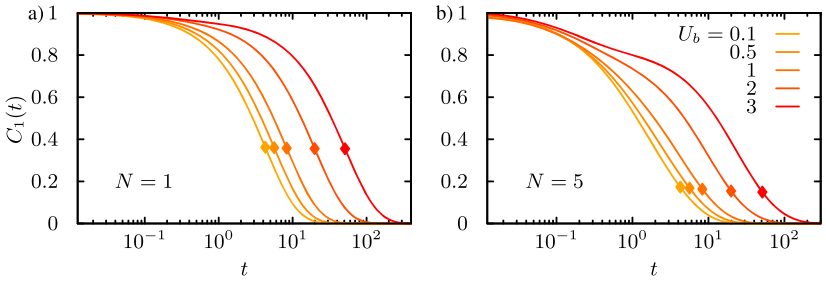

FIG. 2. Position autocorrelation function $C_1(t)$ of an isolated particle (a) and the leftmost tagged-particle in a single file with five particles (b) as a function of the barrier height U_b. Symbols denote $C_1(\Lambda_1^{-1})$.

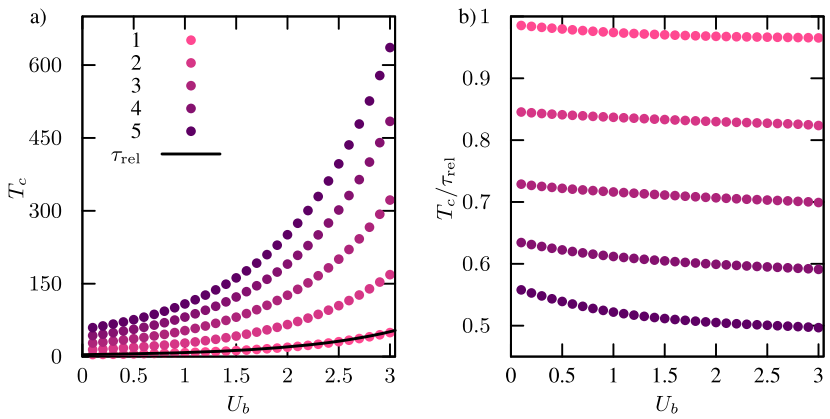

FIG. 3. (a) T_c (in units of collision time) for the first particle (i.e., i = 1) as a function of the barrier height U_b for various values of N. The full line depicts $\tau_{\rm rel} \equiv \Lambda_1^{-1}$ (in absolute time units). (b) Ratio $T_c/\tau_{\rm rel}$ as a function of the barrier height U_b for various values of N; both T_c and $\tau_{\rm rel}$ are measured in units of collision time.

As shown by Zwanzig from first principles,[58,59] one can also analyze the memory encoded in $C_i(t)$ defined in Eq. (10) in terms of a *memory function* $K_U(t)$ defined through

$$\frac{d}{dt}C_i(t) = -\int_0^t K_U(s)C_i(t-s)ds, \tag{14}$$

where the subscript U is included to stress that the memory kernel depends on the external potential. The kinetic equation (14) obeyed *exactly*.[58,59]

Note that the memory kernel $K_U(t)$ in the *linear* kinetic equation (14) is *not* equivalent to the memory kernel entering a *non-linear* generalized Langevin equation for a tagged-particle motion in a potential of mean force.[48,49,59] If, however, one were to compute $C_i(t)$ from such a non-linear generalized Langevin equation, this would yield Eq. (14). Here, we aim to connect quantitatively the different signatures of memory encoded in $C_i(t)$ and the correlation time T_c solely by means of the information encoded in $C_i(t)$. Note that this approach is simple and model-free and can therefore directly be used in the analysis of experimental and simulation data. Alternatively, one may equally well use a non-linear framework (for an excellent recent example, see Ref. 89) that, however, requires more effort and a more detailed input.

We determine $K_U(s)$ from the Laplace transform of Eq. (14),

$$\tilde{K}_U(u) = \frac{1}{\sum_{\mathbf{k}\neq\mathbf{0}} a_{\mathbf{k}}/(\Lambda_{\mathbf{k}}+u)} - u, \tag{15}$$

where $\tilde{f}(u) \equiv \int_0^\infty e^{-ut}f(t)dt$. The inverse Laplace transform is, in turn, determined by numerically inverting Eq. (15) using the *fixed Talbot method*.[90]

By construction, $\int_0^t K_U(s)C_i(t-s)ds \geq 0$, and therefore, $K_U(t)$ must have a positive contribution at least for $t \to 0$. For example, if $C_i(t)$ decays *exactly* as a single exponential with rate Λ, we have $\tilde{K}_U(u) = \Lambda$, and hence, $K_U(t) = \Lambda\delta(t)$. In fact, one can show by means of Mori's projection-operator formalism that $K_U(t)$ has the generic structure $K_U(t) = a\delta(t) + \zeta(t)$, where $a > 0$ and $\zeta(t)$ is a smooth function of t [see, e.g., Eq. (8.61) in Ref. 59].

More generally, when memory is short-lived, that is, when $K(t)$ decays rapidly compared to the timescale on which $C_i(t)$ changes appreciably, we may approximate Eq. (14) as $\frac{d}{dt}C_i(t) \approx -(\int_0^\infty K(s)ds)C_i(t) \equiv -\Lambda C_i(t)$, and hence, the autocorrelation decays approximately as a single exponential $C_i(t) \approx e^{-\Lambda t}$—the system is therefore said to be effectively memoryless (Markovian).[58,59]

The memory kernel of an isolated particle and that of the leftmost tagged-particle in a single file are depicted in Fig. 4 [note that we depict $-K_U(t) > 0$, implying an anti-persistent motion]. The unavoidable truncation of the spectral solution (7) does not allow us to determine $K_U(t)$ in the limit of $t \to 0$. In the case of an isolated particle [Fig. 4(a)], the memory is short-lived and decays on a timescale $t \ll \Lambda_1^{-1}$ much shorter than the relaxation time and decreases with the barrier height U_b. This agrees with the essentially single exponential decay of $C_1(t)$ found in Fig. 2 and implies that the dynamics is essentially memoryless.[58,59]

Conversely, in the case of a tagged-particle [see Fig. 4(b)], $K_U(t)$ displays a strikingly different behavior. First, the range where $K_U(t)$

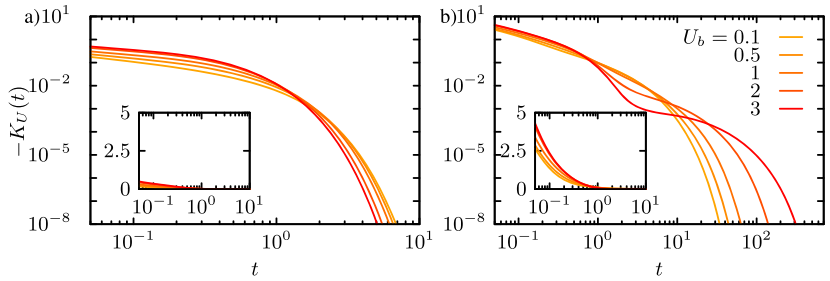

FIG. 4. Memory kernel $-K_U(t)$ of an isolated particle (a) and the leftmost tagged-particle in a single file with five particles (b) as a function of the barrier height U_b shown on a double logarithmic scale. The inset provides the same results shown on a linear-logarithmic scale. We used 900 pairs $a_{\mathbf{k}}$, $\Lambda_{\mathbf{k}}$ to determine $\tilde{K}_U(u)$ in Eq. (15). Note that the range of t in (a) and (b) is different.

considerably differs from zero is orders of magnitude longer and increases with an increase in the barrier height U_b. Second, the anti-persistence of $K_U(t)$ is much larger than for an isolated particle, and third, for high barriers, $K_U(t)$ develops a shoulder, indicating a transiently stalled decay of memory, presumably due to "jamming" in front of the barrier prior to crossing. The latter acts as a transient entropic trap.

Importantly, U_b strongly and non-trivially affects the memory in the tagged-particle's motion [compare with the trivial effect of U_b on $K(t)$ for an isolated particle in Fig. 4(a)]. As a result, any microscopically consistent memory kernel $K_U(t)$ must depend on the external potential $U(x)$. The reason is twofold: (i) the external potential also acts on the background degrees of freedom and (ii) the coupling of the background degrees of freedom and the tagged-particle's motion is strong. In fact, whenever (i) and/or (ii) hold, the external potential generally alters the memory. Conclusive evidence that the potential affects the memory function has been found, e.g., by atomistic computer simulations of molecular solutes in water.[91]

In contrast to $C_1(t)$ depicted in Fig. 2, which on an absolute timescale decays to zero faster for larger N as a result of being normalized and having the same relaxation time Λ_1^{-1}, the memory kernel $K_U(t)$ clearly displays long-time memory effects that become more pronounced as N increases. This can be understood by noting that $K_U(t)$ in Eq. (14) is unaffected by the normalization. The memory kernel is thus more informative than $C_1(t)$ and less ambiguous than correlation times T_c. Moreover, it is not required that $C_i(t)$ is known analytically in order to apply the analysis.

IV. RELAXATION FROM A PINNED CONFIGURATION

We now focus on the "complete" (i.e., including correlations to all orders) relaxation to equilibrium from a *pinned* configuration. That is, we are interested in those initial configurations where either the first ($i = 1$) or the last ($i = N$) particle is pinned at x_0, while the initial conditions of the remaining particles are drawn from the corresponding pinned equilibria (i.e., those equilibrium many-body configurations where the first/last particle is located at x_0). In this non-stationary setting, the analysis of memory kernels seems less sensible since these would depend explicitly on time and x_0.

We quantify the relaxation dynamics by means of $\mathscr{D}(t, x_{0i})$, the Kullback–Leibler divergence[92] between the non-Markovian probability density of the tagged-particle's position at time t, $\mathscr{G}(x_i, t|x_{0i})$ in Eq. (7), and the respective equilibrium density $\mathscr{P}_{\rm eq}(x_i) \equiv \lim_{t\to\infty} \mathscr{G}(x_i, t|x_{0i})$,

$$\mathscr{D}(t, x_{0i}) \equiv \int_{-\pi}^{\pi} dx \mathscr{G}(x, t|x_{0i}) \ln\left(\frac{\mathscr{G}(x, t|x_{0i})}{\mathscr{P}_{\rm eq}(x)}\right). \tag{16}$$

In physical terms, $\mathscr{D}(t, x_{0i})$ represents the displacement from equilibrium in the sense of an *excess instantaneous free energy*, i.e., $k_{\rm B}T\mathscr{D}(t, x_{0i}) = F(t) - F$.[93–95] Since the integral in Eq. (16) cannot be performed analytically, we evaluate it numerically. We always pin the initial position of the tagged-particle at $x_0 = -2$. According to the effect of the pinning on the relaxation of the tagged-particle, the scenario in which we tag the first particle is referred to as "*confining*" (since background particles obstruct the relaxation of the tagged-particle) and the one in which we tag the first particle as "*pushing*" (since background particles exert an entropic force pushing the tagged-particle over the barrier). $\mathscr{D}(t, x_{0i})$ as a function of the barrier height U_b for $N = 5$ and $N = 9$ is shown in Fig. 5.

Note that $\lim_{t\to 0} \mathscr{D}(t, x_{0i}) = \infty$ irrespective of N and U_b since we are comparing a delta distribution with a smooth probability density. Conversely, in an arbitrarily small time interval $\tau_\varepsilon > 0$, the non-Markovian tagged-particle density $\mathscr{G}(x, t|x_{0i})$ evolves to a smooth, well-behaved probability density such that $\mathscr{D}(t > 0, x_{0i})$ is always finite and the "pathology" at $t = 0$ is mathematical and not physical.

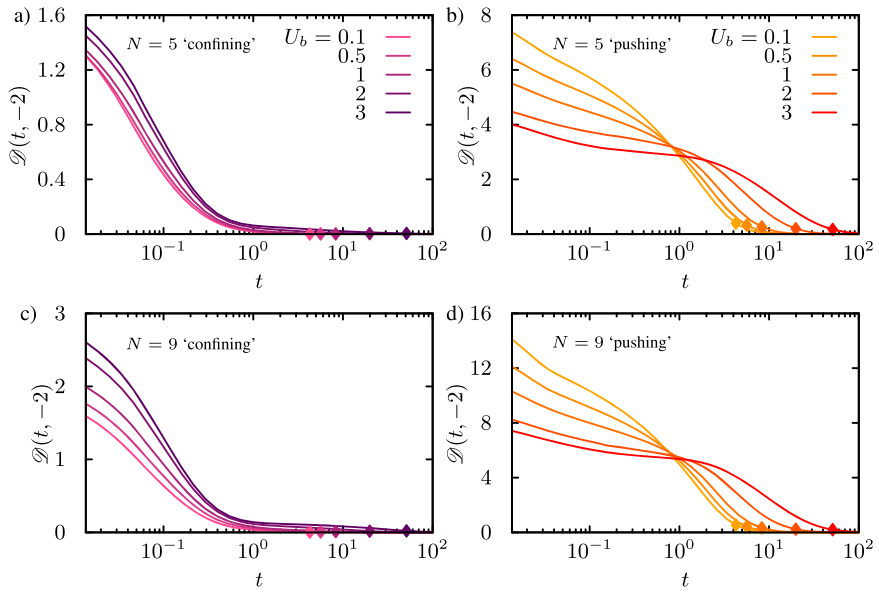

FIG. 5. Time evolution of $\mathscr{D}(t, x_{0i})$ for various barrier heights U_b for $N = 5$ [(a): confining and (b): pushing] and $N = 9$ [(c): confining and (d): pushing], respectively. The symbols denote $\mathscr{D}(\Lambda_1^{-1}, x_{0i})$.

With this in mind, we observe in Fig. 5 a striking difference between the "confining" and "pushing" scenarios. In the "confining" setting, $\mathscr{D}(t, x_{01})$ at a fixed time t is a monotonically increasing function of U_b and as a function of time decays on a timescale that seems to be rather independent of U_b. In the "confining" scenario, an increase in U_b displaces the system at $t = 0^+$ further from equilibrium. This is intuitive because $\mathscr{P}_{\rm eq}(x_1)$ becomes more strongly confined to the boundary and hence away from x_0. To a dominant extent, relaxation occurs already on timescales $t \gtrsim 1 \ll \Lambda_{\mathbf{1}}^{-1}$. The reason may be found in the fact that $\Lambda_{\mathbf{1}}^{-1}$ corresponds to the mixing/ergodic timescale on which the full single file (and thus the tagged-particle) explores the entire system. In the "confining" scenario, the background particles are drawn from a distribution that resembles closely the unconstrained equilibrium, and in addition, the tagged-particle is nominally unlikely to be found in the right well in equilibrium. Therefore, the fraction of paths that cross the barrier in the ensemble of relaxation paths is small, rendering $V_{\mathbf{0k}} V_{\mathbf{k0}}$ for low-lying $\mathbf{k}$ essentially negligible [see Eq. (7)]. Nevertheless, a second, slower relaxation stage is still discernible at $t \gtrsim 1$.

Conversely, in the "pushing" scenario depicted in Figs. 5(b) and 5(d), we find (i) the dependence of $\mathscr{D}(0^+, x_{01})$ on U_b to be inverted, and (ii) for given N and U_b, relaxation extends to much longer timescales compared to the "confining" scenario. In order to rationalize (i), we consider a pair of barriers U_{b_1}, U_{b_2} and take the limit

$$\lim_{t\to 0}\left(\mathscr{D}^{b_1}(t,x_0) - \mathscr{D}^{b_2}(t,x_0)\right) = \ln\left(\mathscr{P}_{\rm eq}^{b_2}(x_0)/\mathscr{P}_{\rm eq}^{b_1}(x_0)\right), \tag{17}$$

which is finite and well defined despite the fact that $\lim_{t\to 0} \mathscr{D}^{b_1,b_2}(t,x_0)$ are infinite. Equation (17) explains that the dependence of $\mathscr{D}(0^+, x_0)$ on U_b is not unique and depends on the pinning point x_0, which determines whether or not $\mathscr{P}_{\rm eq}^{b_2}(x_0)/\mathscr{P}_{\rm eq}^{b_1}(x_0)$ is greater or smaller than 1 [see Figs. 1(b) and 1(d)]. (ii) can be understood by an extension of the argument put forward in the discussion of the "confining" scenario, i.e., as a result of the pinning, the initial configurations of the background particles are displaced much further away from equilibrium, rendering $V_{\mathbf{0k}} V_{\mathbf{k0}}$ for low-lying $\mathbf{k}$ substantial [see Eq. (7)]. Therefore, a pronounced second relaxation stage is visible at longer times $t \gtrsim 1$.

Based on Fig. 5 alone we are not able to deduce whether these observations are a trivial consequence of the pinning in the sense that they have nothing to do with memory (note that a Markov process "remembers" the initial condition up to $\sim\tau_{\rm rel}$) or whether they are, in fact, a signature of memory in the dynamics. Additional insight is gained by inspecting the relaxation of the full, Markovian single file evolving from the same initial condition, i.e.,

$$\mathscr{D}_M(t,x_0) \equiv \left[\prod_{i=1}^{N}\int_{-\pi}^{\pi} dx_i\right] G(\mathbf{x},t,P_0)\ln\left(\frac{G(\mathbf{x},t,P_0)}{P_{\rm eq}(\mathbf{x})}\right), \tag{18}$$

where we have introduced the joint Markovian two-point probability density $G(\mathbf{x}, t, P_0) \equiv \int d\mathbf{y}_0 G(\mathbf{x}, t|\mathbf{y}_0) P_0(\mathbf{y}_0)$, and whereby, for $-\pi < x_0 < -\pi/2$, $P_0(y)$ is defined as

$$P_0(\mathbf{x}) = N!(\pi + x_0)^{-N_L}\hat{O}_{\mathbf{x}}\delta(x_i - x_0)\frac{e^{-U_b\sum_{j=i+1}^{N}\theta(\pi/2-|x_j|)}}{(\pi e^{-U_b} - x_0)^{N_R}}, \tag{19}$$

where $\theta(x)$ is the Heaviside step function and $P_{\rm eq}(\mathbf{x}) = \lim_{t\to\infty} G(\mathbf{x}, t|\mathbf{x}_0)$. The integration in Eq. (18) can be performed analytically (for details, see Ref. 95). Introducing the two-point joint density of the single-particle problem $\Gamma_t(x,a,b) \equiv \sum_k \psi_k^R(x)[\int_a^b dy \psi_k^L(y) P_0(y)]e^{-\lambda_k t}$, with $P_0(y) \equiv \theta(-\pi/2 - y)/(\pi + x_0) + \theta(y + \pi/2)e^{-U(y)}/(\pi e^{-U_b} - x_0)$ and the auxiliary function

$$\Xi_t(a,b) = \int_a^b dx \Gamma_t(x,a,b)\ln(\Gamma_t(x,a,b)/P_{\rm eq}(x)), \tag{20}$$

where $P_{\rm eq}(x) = e^{-U(x)}/\pi(1 + e^{-U_b})$, the result reads

$$\mathscr{D}_M(t,x_0) = \Xi_t(-\pi,\pi)\Xi_t(-\pi,x_0)^{N_L}\Xi_t(x_0,\pi)^{N_R}. \tag{21}$$

An explicit solution is obtained with the aid of Mathematica.[96] As it is bulky, but straightforward, we do not show it here. The Markovian result in Eq. (21) for the same set of parameters, as in Figs. 5(a) and 5(b), is depicted in Fig. 6. A comparison of Figs. 5 and 6 reveals that the second, long-time relaxation stage observed in the "pushing" scenario of Fig. 5 is absent in the Markovian setting (compare Figs. 5 and 6, and note that the relaxation time $\Lambda_{\mathbf{1}}^{-1}$ is identical in both settings). This, in turn, implies that the pronounced second relaxation stage in the non-Markovian, tagged-particle scenario at times $t \gtrsim 1$ is, indeed, a signature of memory.

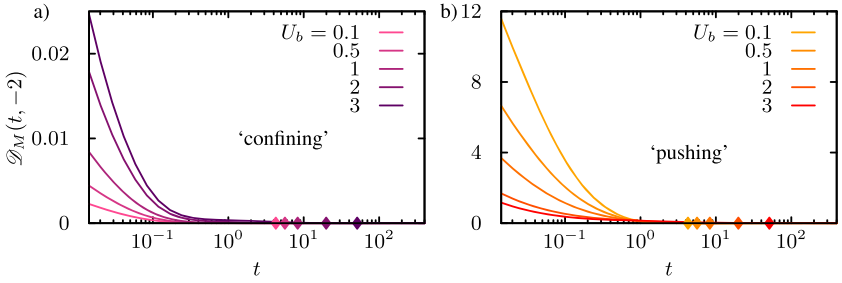

FIG. 6. Time evolution of $\mathscr{D}_M(t, x_{0i})$ for various barrier-heights U_b for $N = 5$ [(a): confining, $i = 1$ and (b): pushing, $i = N$]. The symbols denote $\mathscr{D}_M(\Lambda_{\mathbf{1}}^{-1}, x_{0i})$.

V. DISCUSSION

We identified pronounced signatures of memory in the overdamped relaxation of a tagged-particle in a single file confined to a bi-stable potential. On the level of linear correlations in equilibrium, memory is visible in the form of a multi-scale relaxation of the autocorrelation function (see Fig. 2), a substantial and long-ranged (linear) memory kernel [see Fig. 4(b)], and a seemingly paradoxical shortening of the so-called correlation time T_c (see Fig. 3). The latter was shown to be an artifact of the definition of T_c. When including the complete correlation-structure as encoded in the so-called excess instantaneous free energy [see Eq. (16)], distinctive signatures of memory emerge in the form of a second, late-time relaxation regime.

The memory originates from the fact that the entire single file relaxes to equilibrium in the form of linearly independent many-body eigenmodes, which become projected onto the motion of a tagged-particle.[35,79] The projection couples distinct modes, thus breaking Markovianity and giving rise to memory.[35] It turns out to be very important which particle is tagged. Here, we were only interested in the "confining" (all background particles in front of the tagged-particle) and "pushing" (all background particles behind the tagged-particle) scenarios and found qualitatively different relaxation behaviors. A systematic analysis would be required to understand the intricate details on how the number of particles on each side affects relaxation dynamics, which is beyond the scope of the present work.

We have shown that the memory non-trivially depends on the external potential. That is, a tagged-particle was shown to experience the external potential directly (i.e., time-locally) and indirectly through the effect it exerts on the memory kernel. This effect is general—it occurs whenever the potential is sufficiently strong and also acts on either the latent degrees of freedom (i.e., those that are integrated out) or the interaction between the tagged-particle and the latent degrees of freedom that is not harmonic or, more generally, non-negligible. Direct evidence for the effect has been found in all-atom computer simulations of the hydration of molecular solutes.[91] It is important to keep this in mind when applying generalized Langevin equations (GLEs) with phenomenological memory kernels or microscopically consistent GLEs "decorated" with an external potential as these may lead to erroneous conclusions or misinterpretations.

The application of the methodology for extracting and analyzing memory in tagged-particle dynamics put forward in Eqs. (10), (14), and (16) requires neither $C_i(t)$ nor $\mathscr{G}(x,t|x_{0i})$ to be known analytically. The quantities can be equally well determined from experiments or computer simulations. The analysis is expected to provide insight into memory effects as long as either the "crowding" (i.e., the concentration of background particles) and/or the barrier-height can be controlled. The qualitative features of the signatures of memory are expected to be preserved in most systems of effectively one-dimensional systems with obstructed tagged-particle dynamics. The proposed analysis of memory effects can be viewed as complementary to the analysis of anomalies in tagged-particle diffusion.[97–99]

Our results can readily be tested by existing experiments probing colloidal particle systems (see, e.g., Refs. 100–102) and may, furthermore, be relevant for a theoretical description of transport in ion-channels.[103–106] Our results can be extended in diverse ways, most immediately by including other types of inter-particle interactions[81] and time-dependent energy barriers.[107]

SUPPLEMENTARY MATERIAL

See the supplementary material for the extension of the code published in Ref. 84 that implements the analytical results presented this article.

ACKNOWLEDGMENTS

The financial support from the German Research Foundation (DFG) through the Emmy Noether Program [Grant No. GO 2762/1-1 (to A.G.)] is gratefully acknowledged. The authors thank Kristian Blom for fruitful discussions.

APPENDIX: SINGLE PARTICLE EIGENSPECTRUM

In this appendix, we give explicit expressions for the single-particle eigenfunctions that are required in the diagonalization of the many-body Fokker–Planck operator using the so-called coordinate Bethe ansatz. For details of the solution method, see Refs. 35, 79, and 84. The eigenfunctions of the corresponding single-particle eigenvalue problem are

$$\begin{aligned}(\partial_x^2 + \partial_x\{\partial_x U(x)\})\psi_k^R(x) &= -\lambda_k\psi_k^R(x),\\ (\partial_x^2 - \{\partial_x U(x)\}\partial_x)\psi_k^L(x) &= -\lambda_k\psi_k^L(x),\end{aligned} \tag{A1}$$

where $\psi_k^{L,R}(x) : [-\pi,\pi] \to \mathbb{R}$ allow for a spectral decomposition of the single-particle Green's function,

$$\Gamma(x,t|x_0) = \sum_k \psi_k^R(x)\psi_k^L(x_0)\mathrm{e}^{-\lambda_k t}. \tag{A2}$$

$\psi_k^{L,R}(x)$ enter Eq. (5) and are here defined via their "Hermitianized" counterpart $\psi_k(x) : [-\pi,\pi] \to \mathbb{R}$ as $\psi_k^R(x) = \mathrm{e}^{-U(x)/2}\psi_k(x)$ and $\psi_k^L(x) = \mathrm{e}^{U(x)/2}\psi_k(x)$, where[108]

$$\psi_k(x) = \sqrt{\frac{2}{1+\delta_{k,0}}}\frac{\mathrm{e}^{-U(x)/2}}{\sqrt{\pi(1+\mathrm{e}^{-f0})}}\cos(\sqrt{\lambda_k}x), \qquad \mathrm{mod}\ (k,4) = 0, \tag{A3}$$

$$\psi_k(x) = \begin{cases} -\dfrac{\cos(\sqrt{\lambda_k}(x+\pi))}{\sqrt{\pi}}, & x < -\pi/2\\ \dfrac{\sin(\sqrt{\lambda_k}x)}{\sqrt{\pi}}, & |x| \le \pi/2\\ \dfrac{\cos(\sqrt{\lambda_k}(x-\pi))}{\sqrt{\pi}}, & x > \pi/2 \end{cases}, \qquad \mathrm{mod}\ (k,4) = 1, \tag{A4}$$

$$\psi_k(x) = \sqrt{2}\frac{\mathrm{e}^{U(x)/2}}{\sqrt{\pi(1+\mathrm{e}^{f0})}}\cos(\sqrt{\lambda_k}x), \qquad \mathrm{mod}\ (k,4) = 2, \tag{A5}$$

$$\psi_k(x) = \begin{cases} \dfrac{\cos(\sqrt{\lambda_k}(x+\pi))}{\sqrt{\pi}}, & x < -\pi/2 \\ \dfrac{\sin(\sqrt{\lambda_k}x)}{\sqrt{\pi}}, & |x| \le \pi/2\,, \\ -\dfrac{\cos(\sqrt{\lambda_k}(x-\pi))}{\sqrt{\pi}}, & x > \pi/2 \end{cases} \qquad \mathrm{mod}\ (k,4) = 3, \tag{A6}$$

where $\delta_{k,0}$ is the Kronecker delta.

DATA AVAILABILITY

The data that support the findings of this study are available from the corresponding author upon reasonable request.

REFERENCES

[1] H. A. Kramers, "Brownian motion in a field of force and the diffusion model of chemical reactions," Physica **7**(4), 284–304 (1940).
[2] A. Nitzan, P. Ortoleva, J. Deutch, and J. Ross, "Fluctuations and transitions at chemical instabilities: The analogy to phase transitions," J. Chem. Phys. **61**(3), 1056–1074 (1974).
[3] F. Schlögl, "Chemical reaction models for non-equilibrium phase transitions," Z. Phys. **253**(2), 147–161 (1972).
[4] I. Matheson, D. F. Walls, and C. W. Gardiner, "Stochastic models of firstorder nonequilibrium phase transitions in chemical reactions," J. Stat. Phys. **12**(1), 21–34 (1975).
[5] R. Landauer, "The role noise in negative resistance circuits," J. Phys. Soc. Jpn. **41**(2), 695–696 (1976).
[6] H. Risken, "Distribution- and correlation-functions for a laser amplitude," Z. Phys. **186**(1), 85–98 (1965).
[7] R. Kubo, K. Matsuo, and K. Kitahara, "Fluctuation and relaxation of macrovariables," J. Stat. Phys. **9**(1), 51–96 (1973).
[8] H. Lannon, J. S. Haghpanah, J. K. Montclare, E. Vanden-Eijnden, and J. Brujic, "Force-clamp experiments reveal the free-energy profile and diffusion coefficient of the collapse of protein molecules," Phys. Rev. Lett. **110**(12), 128301 (2013).
[9] H. S. Chung and W. A. Eaton, "Protein folding transition path times from single molecule FRET," Curr. Opin. Struct. Biol. **48**, 30–39 (2018).
[10] H. Yu, A. N. Gupta, X. Liu, K. Neupane, A. M. Brigley, I. Sosova, and M. T. Woodside, "Energy landscape analysis of native folding of the prion protein yields the diffusion constant, transition path time, and rates," Proc. Natl. Acad. Sci. U. S. A. **109**(36), 14452–14457 (2012).
[11] A. P. Manuel, J. Lambert, and M. T. Woodside, "Reconstructing folding energy landscapes from splitting probability analysis of single-molecule trajectories," Proc. Natl. Acad. Sci. U. S. A. **112**(23), 7183–7188 (2015).
[12] K. Truex, H. S. Chung, J. M. Louis, and W. A. Eaton, "Testing landscape theory for biomolecular processes with single molecule fluorescence spectroscopy," Phys. Rev. Lett. **115**(1), 018101 (2015).
[13] H. S. Chung, K. McHale, J. M. Louis, and W. A. Eaton, "Single-molecule fluorescence experiments determine protein folding transition path times," Science **335**(6071), 981–984 (2012).
[14] D. de Sancho, A. Sirur, and R. B. Best, "Molecular origins of internal friction effects on protein-folding rates," Nat. Commun. **5**(1), 4307 (2014).
[15] R. Best and G. Hummer, "Diffusive model of protein folding dynamics with Kramers turnover in rate," Phys. Rev. Lett. **96**(22), 228104 (2006).
[16] J. Kappler, J. O. Daldrop, F. N. Brünig, M. D. Boehle, and R. R. Netz, "Memory-induced acceleration and slowdown of barrier crossing," J. Chem. Phys. **148**(1), 014903 (2018).
[17] K. Neupane, A. P. Manuel, J. Lambert, and M. T. Woodside, "Transition-path probability as a test of reaction-coordinate quality reveals DNA hairpin folding is a one-dimensional diffusive process," J. Phys. Chem. Lett. **6**(6), 1005–1010 (2015).
[18] K. Neupane, D. A. N. Foster, D. R. Dee, H. Yu, F. Wang, and M. T. Woodside, "Direct observation of transition paths during the folding of proteins and nucleic acids," Science **352**(6282), 239–242 (2016).
[19] F. Rico, A. Russek, L. González, H. Grubmüller, and S. Scheuring, "Heterogeneous and rate-dependent streptavidin-biotin unbinding revealed by high-speed force spectroscopy and atomistic simulations," Proc. Natl. Acad. Sci. U. S. A. **116**(14), 6594–6601 (2019).
[20] N. G. van Kampen, "A soluble model for diffusion in a bistable potential," J. Stat. Phys. **17**(2), 71–88 (1977).
[21] B. Caroli, C. Caroli, and B. Roulet, "Diffusion in a bistable potential: A systematic WKB treatment," J. Stat. Phys. **21**(4), 415–437 (1979).
[22] Y. Saito, "Relaxation in a bistable system," J. Phys. Soc. Jpn. **41**(2), 388–393 (1976).
[23] A. Bunde and J.-F. Gouyet, "Brownian motion in the bistable potential at intermediate and high friction: Relaxation from the instability point," Physica A **132**(2), 357–374 (1985).
[24] P. Hanggi, H. Grabert, P. Talkner, and H. Thomas, "Bistable systems: Master equation versus Fokker-Planck modeling," Phys. Rev. A **29**, 371–378 (1984).
[25] A. Perico, R. Pratolongo, K. F. Freed, R. W. Pastor, and A. Szabo, "Positional time correlation function for one-dimensional systems with barrier crossing: Memory function corrections to the optimized Rouse–Zimm approximation," J. Chem. Phys. **98**(1), 564–573 (1993).
[26] A. Perico, R. Pratolongo, K. F. Freed, and A. Szabo, "Torsional time correlation function for one-dimensional systems with barrier crossing: Periodic potential," J. Chem. Phys. **101**(3), 2554–2561 (1994).
[27] P. Hänggi, P. Talkner, and M. Borkovec, "Reaction-rate theory: Fifty years after Kramers," Rev. Mod. Phys. **62**(2), 251–341 (1990).
[28] B. U. Felderhof, "Escape by diffusion from a square well across a square barrier," Physica A **387**(1), 39–56 (2008).
[29] V. Berdichevsky and M. Gitterman, "One-dimensional diffusion through single- and double-square barriers," J. Phys. A: Math. Gen. **29**(8), 1567–1580 (1996).
[30] B. Jun and D. L. Weaver, "One-dimensional potential barrier model of protein folding with intermediates," J. Chem. Phys. **116**(1), 418 (2002).
[31] G. R. Fleming, S. H. Courtney, and M. W. Balk, "Activated barrier crossing: Comparison of experiment and theory," J. Stat. Phys. **42**(1-2), 83–104 (1986).
[32] A. M. Berezhkovskii and D. E. Makarov, "Communication: Transition-path velocity as an experimental measure of barrier crossing dynamics," J. Chem. Phys. **148**(20), 201102 (2018).
[33] D. Hartich and A. Godec, "Duality between relaxation and first passage in reversible Markov dynamics: Rugged energy landscapes disentangled," New J. Phys. **20**(11), 112002 (2018).
[34] D. Hartich and A. Godec, "Interlacing relaxation and first-passage phenomena in reversible discrete and continuous space Markovian dynamics," J. Stat. Mech.: Theory Exp. **2019**(2), 024002.
[35] A. Lapolla and A. Godec, "Manifestations of projection-induced memory: General theory and the tilted single file," Front. Phys. **7**, 182 (2019).
[36] N. G. van Kampen, "Remarks on non-Markov processes," Braz. J. Phys. **28**(2), 90–96 (1998).
[37] H. Peter and F. Mojtabai, "Thermally activated escape rate in presence of long-time memory," Phys. Rev. A **26**(2), 1168–1170 (1982).
[38] S. Okuyama and D. W. Oxtoby, "The generalized Smoluchowski equation and non-Markovian dynamics," J. Chem. Phys. **84**(10), 5824–5829 (1986).
[39] S. Okuyama and D. W. Oxtoby, "Non-Markovian dynamics and barrier crossing rates at high viscosity," J. Chem. Phys. **84**(10), 5830–5835 (1986).
[40] B. Carmeli and A. Nitzan, "Non-Markoffian theory of activated rate processes," Phys. Rev. Lett. **49**(7), 423–426 (1982).
[41] B. Carmeli and A. Nitzan, "Non-Markovian theory of activated rate processes. I. Formalism," J. Chem. Phys. **79**(1), 393–404 (1983).
[42] B. Carmeli and A. Nitzan, "Non-Markovian theory of activated rate processes. IV. The double well model," J. Chem. Phys. **80**(8), 3596–3605 (1984).

[43]V. I. Mel'nikov and S. V. Meshkov, "Theory of activated rate processes: Exact solution of the Kramers problem," J. Chem. Phys. **85**(2), 1018–1027 (1986).
[44]Y. P. Kalmykov, W. T. Coffey, and S. V. Titov, "Thermally activated escape rate for a Brownian particle in a double-well potential for all values of the dissipation," J. Chem. Phys. **124**(2), 024107 (2006).
[45]R. F. Grote and J. T. Hynes, "The stable states picture of chemical reactions. II. Rate constants for condensed and gas phase reaction models," J. Chem. Phys. **73**(6), 2715–2732 (1980).
[46]D. Chandler, "Statistical mechanics of isomerization dynamics in liquids and the transition state approximation," J. Chem. Phys. **68**(6), 2959 (1978).
[47]R. Chakrabarti, "Exact analytical evaluation of time dependent transmission coefficient from the method of reactive flux for an inverted parabolic barrier," J. Chem. Phys. **126**(13), 134106 (2007).
[48]R. Satija and D. E. Makarov, "Generalized Langevin equation as a model for barrier crossing dynamics in biomolecular folding," J. Phys. Chem. B **123**(4), 802–810 (2019).
[49]D. E. Makarov, "Interplay of non-Markov and internal friction effects in the barrier crossing kinetics of biopolymers: Insights from an analytically solvable model," J. Chem. Phys. **138**(1), 014102 (2013).
[50]J. Kappler, V. B. Hinrichsen, and R. R. Netz, "Non-Markovian barrier crossing with two-time-scale memory is dominated by the faster memory component," Eur. Phys. J. E **42**(9), 119 (2019).
[51]S. L. Seyler and S. Pressé, "Surmounting potential barriers: Hydrodynamic memory hedges against thermal fluctuations in particle transport," J. Chem. Phys. **153**(4), 041102 (2020).
[52]A. G. T. Pyo and M. T. Woodside, "Memory effects in single-molecule force spectroscopy measurements of biomolecular folding," Phys. Chem. Chem. Phys. **21**(44), 24527–24534 (2019).
[53]P. Hänggi, F. Marchesoni, and P. Grigolini, "Bistable flow driven by coloured Gaussian noise: A critical study," Z. Phys. B: Condens. Matter **56**(4), 333–339 (1984).
[54]P. Hänggi, "Path integral solutions for non-Markovian processes," Z. Phys. B: Condens. Matter **75**(2), 275–281 (1989).
[55]R. F. Fox, "Functional-calculus approach to stochastic differential equations," Phys. Rev. A **33**, 467–476 (1986).
[56]C. R. Doering, P. S. Hagan, and C. D. Levermore, "Bistability driven by weakly colored Gaussian noise: The Fokker-Planck boundary layer and mean first-passage times," Phys. Rev. Lett. **59**, 2129–2132 (1987).
[57]J. Casademunt, R. Mannella, P. V. E. McClintock, F. E. Moss, and J. M. Sancho, "Relaxation times of non-Markovian processes," Phys. Rev. A **35**, 5183–5190 (1987).
[58]R. Zwanzig, "Statistical mechanics of irreversibility," in *Lectures in Theoretical Physiscs* (Wiley, New York, 1961), p. 106.
[59]R. Zwanzig, *Nonequilibrium Statistical Mechanics* (Oxford University Press, 2004).
[60]G. Hummer, J. C. Rasaiah, and J. P. Noworyta, "Water conduction through the hydrophobic channel of a carbon nanotube," Nature **414**(6860), 188–190 (2001).
[61]T. Chou and D. Lohse, "Entropy-driven pumping in zeolites and biological channels," Phys. Rev. Lett. **82**(17), 3552–3555 (1999).
[62]S. Ahlberg, T. Ambjörnsson, and L. Lizana, "Many-body effects on tracer particle diffusion with applications for single-protein dynamics on DNA," New J. Phys. **17**(4), 043036 (2015).
[63]G.-W. Li, O. G. Berg, and J. Elf, "Effects of macromolecular crowding and DNA looping on gene regulation kinetics," Nat. Phys. **5**(4), 294–297 (2009).
[64]P. M. Richards, "Theory of one-dimensional hopping conductivity and diffusion," Phys. Rev. B **16**(4), 1393–1409 (1977).
[65]A. Taloni, O. Flomenbom, R. Castañeda-Priego, and F. Marchesoni, "Single file dynamics in soft materials," Soft Matter **13**(6), 1096–1106 (2017).
[66]C. Lutz, M. Kollmann, and C. Bechinger, "Single-file diffusion of colloids in one-dimensional channels," Phys. Rev. Lett. **93**, 026001 (2004).
[67]B. Lin, M. Meron, B. Cui, S. A. Rice, and H. Diamant, "From random walk to single-file diffusion," Phys. Rev. Lett. **94**, 216001 (2005).
[68]E. Locatelli, M. Pierno, F. Baldovin, E. Orlandini, Y. Tan, and S. Pagliara, "Single-file escape of colloidal particles from microfluidic channels," Phys. Rev. Lett. **117**, 038001 (2016).
[69]T. E. Harris, "Diffusion with 'collisions' between particles," J. Appl. Probab. **2**(2), 323–338 (1965).
[70]D. W. Jepsen, "Dynamics of a simple many-body system of hard rods," J. Math. Phys. **6**(3), 405–413 (1965).
[71]L. Lizana and T. Ambjörnsson, "Single-file diffusion in a box," Phys. Rev. Lett. **100**(20), 200601 (2008).
[72]L. Lizana and T. Ambjörnsson, "Diffusion of finite-sized hard-core interacting particles in a one-dimensional box: Tagged particle dynamics," Phys. Rev. E **80**(5), 051103 (2009).
[73]E. Barkai and R. Silbey, "Theory of single file diffusion in a force field," Phys. Rev. Lett. **102**(5), 050602 (2009).
[74]E. Barkai and R. Silbey, "Diffusion of tagged particle in an exclusion process," Phys. Rev. E **81**(4), 041129 (2010).
[75]N. Leibovich and E. Barkai, "Everlasting effect of initial conditions on single-file diffusion," Phys. Rev. E **88**(3), 032107 (2013).
[76]O. Flomenbom and A. Taloni, "On single-file and less dense processes," Europhys. Lett. **83**(2), 20004 (2008).
[77]R. Metzler, L. Sanders, M. A. Lomholt, L. Lizana, K. Fogelmark, and T. Ambjörnsson, "Ageing single file motion," Eur. Phys. J.: Spec. Top. **223**(14), 3287–3293 (2014).
[78]L. Lizana, T. Ambjörnsson, A. Taloni, E. Barkai, and M. A. Lomholt, "Foundation of fractional Langevin equation: Harmonization of a many-body problem," Phys. Rev. E **81**(5), 051118 (2010).
[79]A. Lapolla and A. Godec, "Unfolding tagged particle histories in single-file diffusion: Exact single- and two-tag local times beyond large deviation theory," New J. Phys. **20**(11), 113021 (2018).
[80]S. D. Goldt and E. M. Terentjev, "Role of the potential landscape on the single-file diffusion through channels," J. Chem. Phys. **141**(22), 224901 (2014).
[81]M. Kollmann, "Single-file diffusion of atomic and colloidal systems: Asymptotic laws," Phys. Rev. Lett. **90**, 180602 (2003).
[82]M. Morsch, H. Risken, and H. D. Vollmer, "One-dimensional diffusion in soluble model potentials," Z. Phys. B: Condens. Matter Quanta **32**(2), 245–252 (1979).
[83]H. Risken and T. Frank, *The Fokker-Planck Equation: Methods of Solution and Applications*, Springer Series in Synergetics, 2nd ed. (Springer-Verlag, Berlin, Heidelberg, 1996).
[84]A. Lapolla and A. Godec, "BetheSF: Efficient computation of the exact tagged-particle propagator in single-file systems via the Bethe eigenspectrum," Comput. Phys. Commun. **258**, 107569 (2021).
[85]See https://www.boost.org/doc/libs/1_71_0/libs/math/doc/html/quadrature.html for details about the quadrature library used; accessed 20 Septemer 2019.
[86]Note that Eqs. (5)–(9) imply that a_k is a positive constant times the square of a real number.
[87]G. Lipari and A. Szabo, "Model-free approach to the interpretation of nuclear magnetic resonance relaxation in macromolecules. 1. Theory and range of validity," J. Am. Chem. Soc. **104**(17), 4546–4559 (1982).
[88]Note that τ_{rel} does not depend on N.
[89]E. Herrera-Delgado, J. Briscoe, and P. Sollich, "Tractable nonlinear memory functions as a tool to capture and explain dynamical behaviors," Phys. Rev. Res. **2**, 043069 (2020).
[90]J. Abate and P. P. Valkó, "Multi-precision Laplace transform inversion," Int. J. Numer. Methods Eng. **60**(5), 979–993 (2004).
[91]J. O. Daldrop, B. G. Kowalik, and R. R. Netz, "External potential modifies friction of molecular solutes in water," Phys. Rev. X **7**, 041065 (2017).
[92]S. Kullback and R. A. Leibler, "On information and sufficiency," Ann. Math. Stat. **22**(1), 79–86 (1951).
[93]M. C. Mackey, "The dynamic origin of increasing entropy," Rev. Mod. Phys. **61**(4), 981–1015 (1989).
[94]H. Qian, "A decomposition of irreversible diffusion processes without detailed balance," J. Math. Phys. **54**(5), 053302 (2013).

[95]A. Lapolla and A. Godec, "Faster uphill relaxation in thermodynamically equidistant temperature quenches," Phys. Rev. Lett. **125**, 110602 (2020).
[96]Wolfram Research, Inc. Mathematica, Version 12.0, 2019.
[97]Y. Meroz, I. M. Sokolov, and J. Klafter, "Test for determining a subdiffusive model in ergodic systems from single trajectories," Phys. Rev. Lett. **110**, 090601 (2013).
[98]M. Schwarzl, A. Godec, and R. Metzler, "Quantifying non-ergodicity of anomalous diffusion with higher order moments," Sci. Rep. **7**(1), 3878 (2017).
[99]R. Metzler, J.-H. Jeon, A. G. Cherstvy, and E. Barkai, "Anomalous diffusion models and their properties: Non-stationarity, non-ergodicity, and ageing at the centenary of single particle tracking," Phys. Chem. Chem. Phys. **16**(44), 24128–24164 (2014).
[100]Q.-H. Wei, C. Bechinger, and P. Leiderer, "Single-file diffusion of colloids in one-dimensional channels," Science **287**(5453), 625–627 (2000).
[101]R. D. L. Hanes, C. Dalle-Ferrier, M. Schmiedeberg, M. C. Jenkins, and S. U. Egelhaaf, "Colloids in one dimensional random energy landscapes," Soft Matter **8**(9), 2714 (2012).
[102]A. L. Thorneywork, J. Gladrow, Y. Qing, M. Rico-Pasto, F. Ritort, H. Bayley, A. B. Kolomeisky, and U. F. Keyser, "Direct detection of molecular intermediates from first-passage times," Sci. Adv. **6**(18), eaaz4642 (2020).
[103]B. Roux, T. Allen, S. Bernèche, and W. Im, "Theoretical and computational models of biological ion channels," Q. Rev. Biophys. **37**(1), 15–103 (2004).
[104]A. Pohorille, M. A. Wilson, and C. Wei, "Validity of the electrodiffusion model for calculating conductance of simple ion channels," J. Phys. Chem. B **121**(15), 3607–3619 (2017).
[105]W. Kopec, D. A. Köpfer, O. N. Vickery, A. S. Bondarenko, T. L. C. Jansen, B. L. de Groot, and U. Zachariae, "Direct knock-on of desolvated ions governs strict ion selectivity in K+ channels," Nat. Chem. **10**(8), 813–820 (2018).
[106]R. Epsztein, R. M. DuChanois, C. L. Ritt, A. Noy, and M. Elimelech, "Towards single-species selectivity of membranes with subnanometre pores," Nat. Nanotechnol. **15**(6), 426–436 (2020).
[107]E. Subrt and P. Chvosta, "Diffusion in the time-dependent double-well potential," Czech J. Phys. **56**(2), 125–139 (2006).
[108]We here correct typos found in the original publications.